Analyst

Accepted Manuscript

ROYAL SOCIETY OF CHEMISTRY

www.rsc.org/analyst

Journal Name

ARTICLE

Colorimetric Detection of Sequence-Specific MicroRNA Based on Duplex-Specific Nuclease-Assisted Nanoparticle Amplification

Received 00th January 20xx,
Accepted 00th January 20xx

DOI: 10.1039/x0xx00000x

www.rsc.org/

Qian Wang, Ru-Dong Li, Bin-Cheng Yin*, and Bang-Ce Ye*

Developing simple and rapid methods for sequence-specific microRNAs (miRNAs) analysis is imperative to miRNA study and use in clinical diagnosis. We have developed a colorimetric method for miRNA detection based on duplex-specific nuclease (DSN)-assisted signal amplification coupled to aggregation of gold nanoparticles (AuNPs). The proposed method involves two processes: target-mediated probe digestion by DSN enzyme and probe-triggered AuNP aggregation as a switch for signal output. The reaction system consists of a rationally designed probe complex formed by two partly complementary DNA probes, and two sets of different oligonucleotide-modified AuNPs with sequences complementary to one DNA probe in probe complex. In the presence of target miRNA, the probe complex is invaded, resulting in the formation of miRNA-probe heteroduplex as substrate of DSN enzyme, and releasing the other probe to link to the AuNPs. The proposed method allows quantitative detection of miR-122 in the range of 20 pM to 1 nM with detection limit of ~16 pM, and shows an excellent ability to discriminate single-base differences. Moreover, the detection assay can be applied to accurately quantify miR-122 in cancerous cell lysates in excellent agreement with the result from a commercial miRNA detection kit. This method is simple, cost-effective, highly selective, and free of dye label and separation procedures.

1 Introduction

MicroRNAs (miRNAs) are short, endogenous, non-coding ribonucleic acid molecules with a length of 18 to 25 nucleotides. MiRNAs negatively regulate gene expression by base pairing with the 3′untranslated region (UTR) of specific target mRNAs leading to gene inactivation. They play a critical role in physiological and pathological processes, including hematopoietic differentiation, cell cycling, regulation, and metabolism.[1-3] Recently, increasing evidence has verified that aberrant expression of miRNAs is closely associated with the development of a variety of cancers, and their expression patterns in cancers appear to be tissue-specific.[4-7] For example, deviant expressions of miR-192 and miR-215 were reported to be indicative of gastric cancer,[8] miR-141 for prostate cancer,[9] miR-122 for liver cancer,[10] and miR-17-3p and miR-92 for colorectal cancer.[11] Hence, miRNAs have become as potential diagnostic or prognostic/predictive biomarkers in miRNA and physiological studies, and clinical diagnosis as well as designer drug therapy.[12-14]

The intrinsic characteristics of miRNAs such as short length, high sequence homology, susceptibility to degradation, and low abundance, present unique detection challenges compared with other nucleic acids. Many bioanalytical methods have been developed for miRNA detection with absolute or relative quantification, including northern blotting,[15, 16] in situ hybridization,[17, 18] microarray,[19, 20] and PCR-based methods.[21-24] Although the northern blot and in situ hybridization techniques were considered as the standard methods in earlier miRNA profiling, their drawbacks of laborious procedures and low sensitivity have prompted biomedical researchers to establish more convenient approaches for miRNA analysis. Although microarray technology can simutaneously identify many miRNAs with high throughput, it is unsatisfactory due to low sensitivity and specificity. PCR-based methods have been widely used because of their good performance and universality, but the utilization of multiple enzymes, especially in reverse transcription PCR-based methods, results in high experimental cost and design complexity, as well as the need for an thermal cycler to precisely control the reaction temperature. Apart from the above problems, these approaches have the same overall drawbacks; they cannot be applied in point-of-care settings or resource-limited locations. Alternatively, enzyme-assisted isothermal amplification methods[25-31] have shown great promise for "on the spot" miRNAs assays. In particular, our group employed duplex-specific nuclease (DSN) to develop a new signal-amplifying mechanism, duplex-specific nuclease signal amplification (DSNSA), for multiplexed detection of miRNAs.[26] Duplex specific nuclease (DSN), obtained from the

Lab of Biosystem and Microanalysis, Biomedical Nanotechnology Center, State Key Laboratory of Bioreactor Engineering, East China University of Science & Technology, Shanghai, 200237, China
† Corresponding author: Bin-Cheng Yin, Email: binchengyin@ecust.edu.cn; Bang-Ce Ye, Email: bcye@ecust.edu.cn.
Electronic Supplementary Information (ESI) available: [details of any supplementary information available should be included here]. See DOI: 10.1039/x0xx00000x

hepatopancreas of the Kamchatka crab (*Paralithodes camtschaticus*),[32] can hydrolyze double-stranded DNA (dsDNA) or DNA in DNA-RNA heteroduplexes, and is practically inactive toward single-stranded DNA, or single- or double-stranded RNA. Based on this unique property, DSN is very suitable for miRNA analysis via the formation of DNA-RNA heteroduplexes using synthesized a DNA probe.

Mirkin and colleagues first demonstrated that gold nanoparticles (AuNPs) are valuable platforms for ultrasensitive detection of biomolecules by virtue of their size-dependent optical and electronic properties.[33] Owing to their high extinction coefficients and strong distance-dependent optical properties, AuNPs have been attractive and widely applied in developing various colorimetric methods with simplicity, low cost, easy handling, and visual signal output monitored by naked eye.[34-40] In this work, we developed a colorimetric assay for absolute quantification of miRNA based on DSN-assisted nanoparticle amplification. We combined the DSN-assisted enzymatic reaction and AuNPs, to develop a simple and sensitive colorimetric method for specific miRNA detection. A rationally designed probe complex, formed by two partly-complementary DNA probes, can resist DSN enzyme hydrolysis; and disintegrate by invasion of target miRNA. One strand of the probe complex hybridizes with target miRNA forming a DNA-RNA heteroduplex and becoming substrate for the DSN enzyme. The other strand acts as the linker of single-stranded DNA-modified AuNPs and triggers particle aggregation with a concomitant colour change from red to blue. The proposed method provides a quantitative readout proportional to the target concentration in the range of 20 pM to 1 nM with a detection limit of ~16 pM. This colorimetric method is simple, rapid, cost-effective, highly selective, and freedom from the problems encountered in fluorescence detection platforms.

2 Experimental

2.1 Reagents and materials

MiRNAs were synthesized by TaKaRa Biotechnology Co., Ltd. (Dalian, China). DNA probes, and thiol-modified probes were synthesized by Sangon Biotech Co., Ltd. (Shanghai, China). The sequences of synthetic miRNAs and oligoncleotides are listed in Table 1. Duplex-specific nuclease (DSN) from Paralithodes camtschaticus was purchased from Evrogen (Moscow, Russia). RNase Inhibitor was purchased from Thermo Fisher Scientific Co., Ltd. (Waltham, MA, USA). Commercial miRNA detection kit (qRT-PCR kit) and diethylpyrocarbonate (DEPC) treated water were purchased from TaKaRa Biotechnology Co., Ltd. (Dalian, China). Hydrogen tetrachloroaurate(III) trihydrate ($HAuCl_4 \cdot 3H_2O$), trisodium citrate, sodium dodecyl sulfate (SDS), tris (2-carboxyethyl) phosphine (TCEP), and Stain-All were purchased from Sigma-Aldrich, Inc. (Saint Louis, MO, USA). The stocks and buffer solutions in this work were dissolved by 0.1% DEPC-treated water and autoclaved. The tips and tubes used were RNase-free and did not require pretreatment to inactivate RNases. Cell lines including human hepatocellular carcinoma cell lines (BEL-7404), human cervical cancer cell lines (HeLa), human breast cancer cell lines (MDA-MB231), and human prostate carcinoma cell lines (22Rv1), were obtained from the cell bank of type culture collection of the Chinese Academy of Sciences (Shanghai, China).

Table 1. Sequence information for synthetic miRNAs and oligonucleotides used in this study.

Name	Sequence [a] (5'→3')
miR-122	UGGAGUGUGACAAUGGUGUUUG
G-miR-122	UGGAGUGUGACGAUGGUGUUUG
miR-221-5p	ACCUGGCAUACAAUGUAGAUUU
miR-221-3p	AGCUACAUUGUCUGCUGGGUUUC
miR-223	UGUCAGUUUGUCAAAUACCCCA
Probe A-1	TGGAGTGTGGTGTTTG
Probe A-2	ATGGAGTGTGGTGTTTGA
Probe A-3	AATGGAGTGTGGTGTTTGAA
Probe A-4	AAATGGAGTGTTTTGGTGTTTGAA
Probe B	CAAACAC**CATTGT**CACACTCCA
S-1	SH-TTTTTTTTTTCAAACACCA
S-2	CACACTCCATTTTTTTTTT-SH

[a] Underlined characters represent the different bases compared with miR-122 in the tested miRNAs. Red and green characters represent the bases complementary with S-1 and S-2, respectively. Bold and underlined characters in Probe B represent the non-pairing bases of the loop in the probe complex.

2.2 Instrumentation

Ultraviolet visible (UV-vis) absorption spectra were recorded on a microplate reader (BioTek Instruments, Winooski, VT, USA) using a transparent 384-well microplate (Greiner, Germany) in the wavelength range of 400 nm to 800 nm. Real-time PCR experiments were performed on a Bio-Rad CFX 96 PCR instrument (BIO-RAD, USA). Transmission electron microscope (TEM) measurements were collected on a Jeol JEM-2100 instrument (JEOL Ltd., Japan). Digital photographs were taken with a Casio S12 digital camera (Tokyo, Japan).

2.3 Preparation of oligonucleotide-functionalized AuNPs

AuNPs with a diameter of 13 nm and oligonucleotide-functionalized AuNPs were prepared according to the reported methods with minor modification.[41-43] Briefly, 1% (w/v) trisodium citrate solution (3.5 mL) was added to the boiling, vigorously stirred 0.01% $HAuCl_4$ solution. The solution was heated and stirred for 20 min, and then naturally cooled to room temperature. The resultant colloid solution (AuNPs) was filtered with 0.22 μm membrane. Then, AuNPs were pretreated by capping with SDS by adding ~0.05% SDS (wt%) to increase the stability. The thiolated single-stranded DNA (ssDNA) was incubated with 5 mM TCEP for 15 min before mixing with as-prepared AuNPs. An equal volume of NaCl solution (2.0 M) was added quickly dropwise into a mixture containing 10 mM phosphate buffer (pH 7.5), 2 μM thiolated ssDNA, and ~2 nM as-prepared AuNPs, with simultaneously vigorous vortex. The resultant mixture was incubated at room temperature for 2 h. After that, the excess thiolated ssDNA was removed by centrifugation at 10,000 rpm for 10 min at 4 °C. The washing step for ssDNA-AuNP conjugates was repeated five times

to thoroughly remove the unreacted ssDNA, then concentrated and kept in buffer containing 50 mM Tris-HCl (pH 8.0), 5 mM $MgCl_2$.

2.4 Detection procedures of miRNA

The detailed procedure for miRNA detection was as follows. First, 1.5 μM probe complex formed by Probe A and Probe B probes (1:1 concentration ratio) was pretreated by heating at 90 °C for 5 min and slowly cooling to room temperature. Then the above probe complex solution was mixed with 0.15 U DSN (dissolved in 25 mM Tris-HCl, pH 8.0; 50% glycerol), 1 U/μL RNase Inhibitor, and target miRNAs in 1× reaction buffer (50 mM Tris-HCl, pH 8.0; 5 mM $MgCl_2$) with a total volume of 20 μL. The mixture was incubated at 45 °C for 60 min. After the incubation step, 20 μL 10 mM EDTA was added to the above reaction mixture to deactivate DSN. Finally, 60 μL solution containing two sets of ssDNA-modified AuNPs in molar ratio of 1:1 with a concentration of 4.5 nM was added, and incubated at room temperature for 45 min before UV-vis spectral measurement.

2.5 Gel electrophoresis analysis

The resultant products of enzymatic reaction was analyzed by a 20% non-denaturing polyacrylamide gel electrophoresis (PAGE) in 1× TAE solution (40 mM Tris, 20 mM acetic acid, 1 mM EDTA, pH 8.3) at 120 V for ~4 h. After electrophoresis, the gel was washed twice in 30% formamide for 20 min each time; and subsequently the gel was stained in the 1×TAE solution (40 mM Tris, 20 mM acetic acid, 1 mM EDTA, pH 8.3) containing 0.01% Stain-All and 30% formamide for 20 min. Then, the gel was colored with 30% ethanol containing 1% EDTA, and photographed using a Casio S12 digital camera.

2.6 Detection of specific miRNA in cell lysates

Four human cancer cell lines, including BEL-7404, MDA-MB231, HeLa, and 22Rv1, were employed to prepare the biological samples. The cell culture and corresponding cell lysates were prepared according to our previous work.[26,44, 45] The detection of target miR-122 in cell lysates followed the above procedures.

3 Results and discussion

3.1 Working principle of the proposed method

The working principle of the proposed colorimetric method for specific miRNA detection based on DSN-assisted nanoparticle amplification is illustrated in Scheme 1. The reaction system consists of the following components: probe complex formed by Probe A and Probe B, target miRNA, DSN enzyme, and two sets of different ssDNA-modified AuNPs. The probe complex formed by Probe A and Probe B has a conformation similar to that of a molecular beacon with a loop in the middle and hybridization regions at two ends. Probe B is designed to be complementary to target miRNA, and is blocked by hybridization with probe A at the 3' and 5' termini. Probe A is designed to hybridize with the two sets of ssDNAs immobilized in AuNPs, whereas it is also blocked by Probe B. Via rational design of the hybridization length within 10 base pairs between Probe A and Probe B at two ends, the probe complex can resist DSN digestion, because DSN cannot hydrolyse dsDNA shorter than 10 base pairs.[32] In the presence of target miRNA, the probe complex is invaded by target miRNA to form a DSN substrate of Probe B-miRNA heteroduplex. Subsequently, DSN enzyme specifically hydrolyses Probe B in DNA-RNA heteroduplex to release the target miRNA, resulting in a new cycle of target invasion of the probe complex. Upon the completion of each strand-invasion and digestion cycle, more Probe A strands are released to trigger AuNP aggregation and a concomitant color change from red to blue owing to the inter-particle coupled plasmon excitons. The AuNP aggregate exhibits decreased light absorption at 520 nm and increased light absorption at 650 nm, which can be conveniently measured by UV-vis spectroscopy. The absorbance ratio at A_{650}/A_{520} is directly proportional to the concentration of miRNA present, allowing quantitative determination of the target miRNA of interest. On the contrary, when the target miRNA is absent, the probe complex remains intact and the AuNP remains in the dispersed state with no absorbance change.

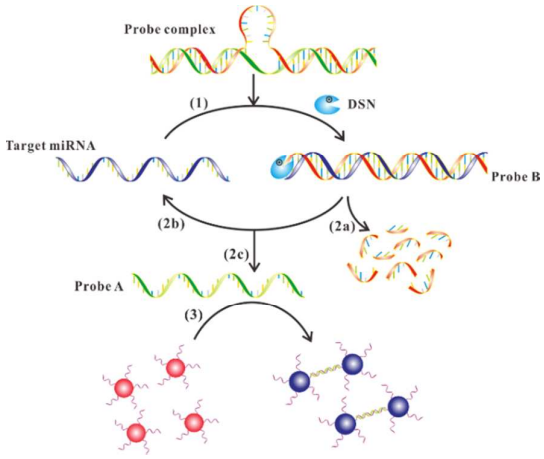

Scheme 1. Schematic illustration of proposed colorimetric method for specific miRNA detection based on DSN-assisted nanoparticle amplification using AuNPs as signal output. Steps (1) indicates the process of target miRNA invasion, (2a) indicates the process of Probe B digestion by DSN, (2b) indicates the process of target miRNA recycle, (2c) indicates the process of Probe A release.

3.2 Feasibility test

We first conducted a non-denaturing polyacrylamide gel electrophoresis (PAGE) assay to test the feasibility of the proposed method in three aspects. First, the probe complex in dsDNA structure must resist hydrolysis by DSN enzyme. Second, the target miRNA must invade the probe complex to hybridize with Probe B and replace the Probe A. Third, the DSN enzyme must hydrolyze Probe B in the Probe B-miRNA heteroduplex. MicroRNA miR-122 was selected as model target. It is a liver specific miRNA, comprising ~70% of the total miRNAs found in the human liver, and is commonly deregulated in liver fibrosis and hepatocellular carcinoma.[10, 46] The probe complex was prepared with a six-base loop in the middle, and nine and seven complementary base pairs at the 5' and 3' ends, respectively formed by Probe A-3 and Probe B. For the feasibility test, the reaction solution containing the probe complex was treated with and

without DSN enzyme or/and miR-122, and incubated at 45 °C for 1 h. After incubation, the resultant solution was tested by non-denaturing PAGE. As shown in Fig. 1, lane 1 and lane 5 are used as controls, containing probe complex and miR-122, respectively. In the presence of DSN enzyme but not miR-122 (lane 2), the probe complex remained intact with no observable degration phenomenon. This strongly confirms the previous results that dsDNA with fewer than ten pairs of complementary nucleotides can resist the digestion of DSN enzyme.[32] When miR-122 is present but not DSN (lane 3), two distinct bands are observed, clearly suggesting that target miRNA efficiently separated the probe complex to release probe A-3. When the mixture of probe complex and miR-122 was treated with DSN enzyme (lane 4), the degradation of Probe B was clearly verified by a smear band (indicated by black square) below the gel. These results clearly verified the feasibility of our proposed method.

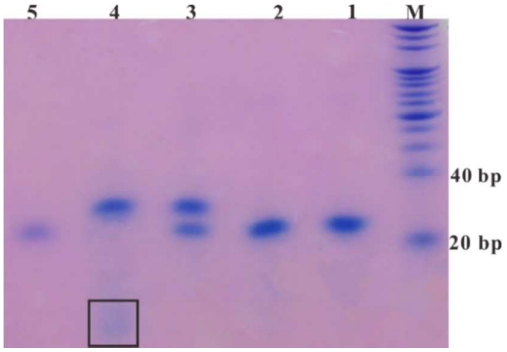

Fig. 1. Non-denaturing PAGE results of the feasibility test of our proposed method. M: DNA marker, lane 1: probe complex, lane 2: probe complex in the presence of DSN enzyme, lane 3: probe complex in the presence of miR-122, lane 4: probe complex in the presence of miR-122 and DSN enzyme, lane 5: miR-122. The concentrations of probe complex, miR-122, DSN enzyme, and RNase Inhibitor in a reaction volume of 20 μL were 500 nM, 50 nM, 0.15 U, and 1 U/μL, respectively.

3.3 Optimization of reaction conditions

Prior to performance investigation of the proposed assay, experimental parameters including the design of Probe A sequence, reaction temperature, the amount of RNase inhibitor, the concentration of probe complex, and reaction time, were thoroughly studied to obtain optimal reaction conditions. The absorbance ratio of 650 nm to 520 nm of AuNPs solution was used to quantitatively evaluate the performance of the test factors. Since Probe A behaves as the inhibitor to Probe B, and at the same time Probe A acts as the linker of the two sets of ssDNA functionalized AuNPs to produce the signal output, we first optimized the hybridization base numbers between Probe A and the AuNP probes (S-1 and S-2). Four types of Probe A were designed with hybridization base numbers with S-1 and S-2 of 8 bp/7 bp (Probe A-1), 8 bp/9 bp (Probe A-2), 10 bp/10 bp (Probe A-3) and 11 bp/11 bp (Probe A-4), respectively. It should be noted that the hybridization length between Probe A and Probe B satisfies the digestion length of DSN enzyme (<10 bp). As shown in Fig. S3, the optimized performance was achieved with Probe A-3. Whereas, Probe A-4 showed the worst signal, which may be due to steric hindrance among Probe A-4, S1, and S2, which negatively impacted AuNP aggregation. In addition, we found that the optimum reaction temperature, the amount of RNase inhibitor, the concentration of probe complex, and the reaction time were 45°C, 1 U/μL, 500 nM, and 60 min, respectively (see Fig. S4-S7 in the Supporting Information). In addition, the characterizations of the prepared AuNPs, ssDNA-modified AuNPs, and the aggregated AuNPs probe triggered by miRNA target were shown in Fig.S1 and Fig.S2.

3.4 Sensitivity investigation

Under the above optimal experimental conditions and according to the experimental protocol described in the Experimental Section, we investigated the sensitivity of the proposed method by detecting synthetic miR-122 at different concentrations (0, 20 pM, 50 pM, 80 pM, 200 pM, 500 pM, 1 nM, and 10 nM) prepared in DEPC-treated water. As expected, a gradual increase in AuNP aggregation was clearly observed with an increase in the concentration of miR-122 from 20 pM to 10 nM, with a color change of the solution from red to faint pale directly observed by the naked eye (Fig. 2A). The color change clearly indicates that Probe A-3 was released from probe complex to trigger AuNP aggregation with a red-shift of the surface plasma absorption peak and corresponding decrease of absorption intensity in the UV–vis spectrum (Fig. 2 B). Fig. 3C inset illustrates that the absorbance ratio of A_{650}/A_{520} exhibited a good linear relationship with the logarithmic (lg) value of miR-122 concentration in the dynamic range from 20 pM to 1 nM. The correlation equation is $A_{650}/A_{520} = 0.192\lg(c_{miR\text{-}122}) - 0.117$ with a regression coefficient R^2 of 0.9512. The detection limit was estimated to be ~16 pM (3σ/S, σ is the standard deviation of the blank solution).

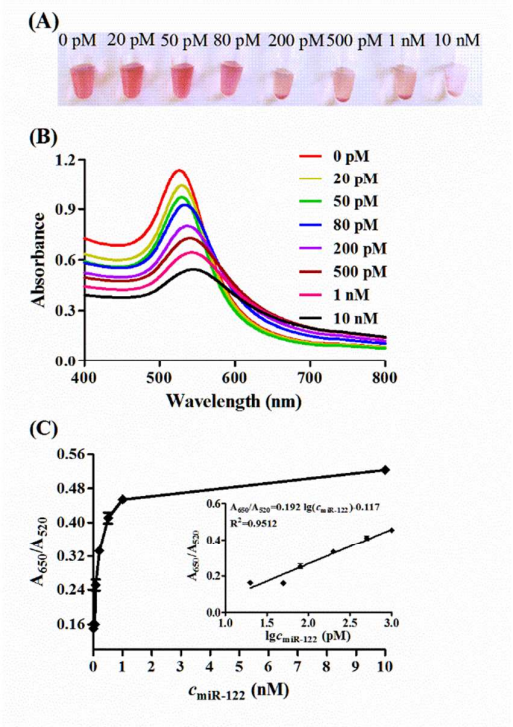

Fig. 2. (A) Digital photograph and (B) absorption spectra of sensing system in response to different concentrations of miR-122. (C)

Absorbance ratio of A_{650}/A_{520} as a function of the concentration of miR-122. Inset: linear-log correlation of the absorbance ratio of A_{650}/A_{520} vs. the base 10 logarithm of miR-122 concentration in the range from 20 pM to 1 nM. Error bars show the standard deviation of three independent experiments.

3.5 Selectivity test

To evaluate the sequence discrimination ability of the proposed assay, we selected miR-122, three other miRNAs associated with hepatocellular carcinoma (miR-221-5p, miR-221-3p, and miR-223), and single-base mismatched miRNA (G-miR-122) compared to miR-122. These synthetic miRNAs were tested at two concentrations (5 nM and 500 pM), respectively. As shown in Fig. 3A, only target miR-122 triggers significant aggregation of AuNPs with precipitate at bottom of tube, while others remain a brilliant red-colored solution of free AuNPs. Correspondingly, the absorbance ratio values of miR-122 are higher than those of non-target sequences at two tested concentrations (Fig. 3B). It should be noticed that G-miR-122 with a single base mutation in the middle also could be clearly differentiated with very low signal, which is due to two reasons. First, the probe complex with a similar structure as a molecular beacon (a loop in the middle and hybridization region at two ends) also has similar function as molecular beacon, that is it can easily distinguish a single base difference. Second, DSN enzyme has the intrinsic property of capable to discriminate between perfectly and non-perfectly matched short DNA-RNA duplex with single-nucleotide mismatch. These results suggest that the specificity of the proposed method is high enough to discriminate between the closely tissue-related miRNAs or miRNA family members with high homology (1- or 2-nt difference).

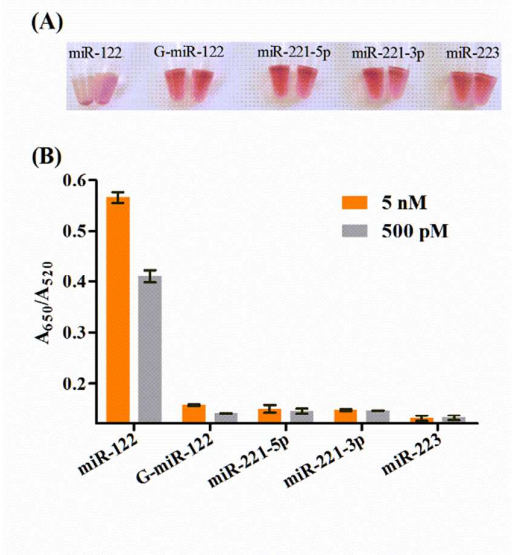

Fig. 3. Selectivity investigation of the proposed method by testing different miRNAs targets. Bars representing absorbance ratio of A_{650}/A_{520} values from the different inputs of miR-122, G-miR-122, miR-221-5p, miR-221-3p, and miR-223 at two concentrations of 5 nM and 500 pM, respectively. Error bars show the standard deviation of three independent experiments.

3.6 Biological sample application

We further investigated the application of proposed method in quantitative detection of miR-122 in a complex biological matrix. The cell lysate samples from four human cancer cell lines, including hepatocellular carcinoma cell lines (BEL-7404), breast cancer cell lines (MDA-MB231), cervical cancer cell lines (HeLa), and prostate carcinoma cell lines (22Rv1), were chosen. We utilized our proposed method and commercial miRNA detection kit to detect the amount of miR-122 in the four tested cell lysates. For comparison, commercial miRNA detection kits based on RT-PCR was used to detect a series of miR-122 standards containing known concentrations to establish a calibration curve (Fig. S8). As shown in Fig. 4, the proposed method worked well in the cell media, and the amounts of miR-122 measured by our proposed method had good accordance with the commercial kit. In addition, the results show that miR-122 had different expression levels in different cancer cell lines. The cell lysate from BEL-7404 hepatocellular carcinoma cells had a higher concentration of miR-122 than that of other tissue cells, which was in good accordance with a previous report of the specific expression of miR-122 in liver tissue.[10, 46] In addition, the accuracy of the proposed method was tested by spiking different concentrations of miR-122 into the BEL-7404 cell lysates. The experimental data listed in Table S1 revealed good recovery rates of standard addition from 101.01 to 103.13%. These results indicate that the proposed method based on DSN assisted nanoparticle amplification has a potential in practical application for miRNAs analysis.

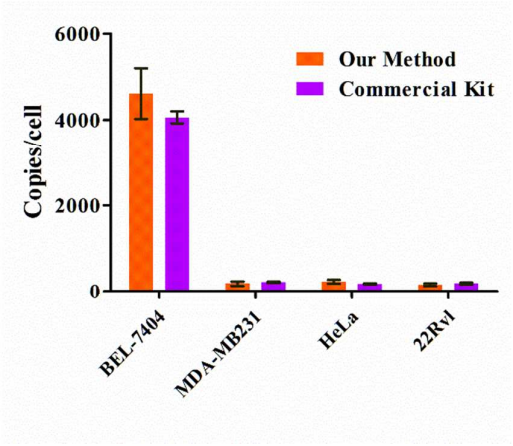

Fig. 4. Practical application test of miR-122 in cancer cell lysates of BEL-7404, MDA-MB231, HeLa, and 22Rv1. Bars represent the detected amount of miR-122 using our proposed method (orange bars) and commercial miRNA detection kit (purple bars), respectively. Error bars show the standard deviation of three independent experiments.

4 Conclusions

We have developed a colorimetric method for sequence-specific miRNA detection based on DSN-assisted nanoparticle amplification with good sensitivity, selectivity, and stability. This method relies upon the unique structure of probe complex, which could resist the degradation of DSN enzyme, and unique property of DSN enzyme on RNA-DNA heteroduplex. The coupling of ssDNA-modified AuNPs as signal readout provides a stable and cost-effective platform, eliminating the need for costly and time-consuming dye

labeling. Based the above distinctive features, we believe that the proposed assay would have great potential as a routine tool for rapid miRNA analysis in ordinary laboratory studies and clinical diagnosis.

Acknowledgements

This work was jointly supported by the National Natural Science Foundation of China (Grants 21335003, 21205040), the Science Fund for Creative Research Groups (21421004), the Key Grant Project of Chinese Ministry of Education (Grant 313019), the Shanghai Fund (12ZR1442700), the Fundamental Research Funds for the Central Universities, and Hitachi, Ltd.

Notes and references

1. D. P. Bartel, *Cell*, 2004, **116**, 281-297.
2. V. Ambros, *Nature*, 2004, **431**, 350-355.
3. B. David P, *Cell*, 2004, **116**, 281-297.
4. A. Esquela-Kerscher and F. J. Slack, *Nat. Rev. Cancer*, 2006, **6**, 259-269.
5. G. A. Calin and C. M. Croce, *Nat. Rev. Cancer*, 2006, **6**, 857-866.
6. A. Keller, P. Leidinger, A. Bauer, A. Elsharawy, J. Haas, C. Backes, A. Wendschlag, N. Giese, C. Tjaden, K. Ott, J. Werner, T. Hackert, K. Ruprecht, H. Huwer, J. Huebers, G. Jacobs, P. Rosenstiel, H. Dommisch, A. Schaefer, J. Muller-Quernheim, B. Wullich, B. Keck, N. Graf, J. Reichrath, B. Vogel, A. Nebel, S. U. Jager, P. Staehler, I. Amarantos, V. Boisguerin, C. Staehler, M. Beier, M. Scheffler, M. W. Buchler, J. Wischhusen, S. F. Haeusler, J. Dietl, S. Hofmann, H. P. Lenhof, S. Schreiber, H. A. Katus, W. Rottbauer, B. Meder, J. D. Hoheisel, A. Franke and E. Meese, *Nat. Methods*, 2011, **8**, 841-843.
7. J. Lu, G. Getz, E. A. Miska, E. Alvarez-Saavedra, J. Lamb, D. Peck, A. Sweet-Cordero, B. L. Ebert, R. H. Mak, A. A. Ferrando, J. R. Downing, T. Jacks, H. R. Horvitz and T. R. Golub, *Nature*, 2005, **435**, 834-838.
8. Z. Jin, F. M. Selaru, Y. Cheng, T. Kan, R. Agarwal, Y. Mori, A. V. Olaru, J. Yang, S. David, J. P. Hamilton, J. M. Abraham, J. Harmon, M. Duncan, E. A. Montgomery and S. J. Meltzer, *Oncogene*, 2011, **30**, 1577-1585.
9. P. S. Mitchell, R. K. Parkin, E. M. Kroh, B. R. Fritz, S. K. Wyman, E. L. Pogosova-Agadjanyan, A. Peterson, J. Noteboom, K. C. O'Briant, A. Allen, D. W. Lin, N. Urban, C. W. Drescher, B. S. Knudsen, D. L. Stirewalt, R. Gentleman, R. L. Vessella, P. S. Nelson, D. B. Martin and M. Tewari, *Proc. Natl. Acad. Sci. U.S.A.* , 2008, **105**, 10513-10518.
10. J. Chang, E. Nicolas, D. Marks, C. Sander, A. Lerro, M. A. Buendia, C. Xu, W. S. Mason, T. Moloshok, R. Bort, K. S. Zaret and J. M. Taylor, *RNA Biol.*, 2004, **1**, 106-113.
11. E. K. Ng, W. W. Chong, H. Jin, E. K. Lam, V. Y. Shin, J. Yu, T. C. Poon, S. S. Ng and J. J. Sung, *Gut*, 2009, **58**, 1375-1381.
12. J. G. Hacia, L. C. Brody, M. S. Chee, S. P. Fodor and F. S. Collins, *Nat. Genet.*, 1996, **14**, 441-447.
13. F. S. Santiago, A. V. Todd, N. J. Hawkins and R. L. Ward, *Mol. Cell. Probes*, 1997, **11**, 33-38.
14. C. Arenz, *Angew. Chem., Int, Ed.*, 2006, **45**, 5048-5050.
15. M. Lagos-Quintana, R. Rauhut, W. Lendeckel and T. Tuschl, *Science*, 2001, **294**, 853-858.
16. A. Válóczi, C. Hornyik, N. Varga, J. Burgyán, S. Kauppinen and Z. Havelda, *Nucleic Acids Res.*, 2004, **32**, e175.
17. J. T. G. Pena, C. Sohn-Lee, S. H. Rouhanifard, J. Ludwig, M. Hafner, A. Mihailovic, C. Lim, D. Holoch, P. Berninger, M. Zavolan and T. Tuschl, *Nat. Methods*, 2009, **6**, 139-141.
18. J. Lu and A. Tsourkas, *Nucleic Acids Res.*, 2009, **37**, e100.
19. L. P. Lim, N. C. Lau, P. Garrett-Engele, A. Grimson, J. M. Schelter, J. Castle, D. P. Bartel, P. S. Linsley and J. M. Johnson, *Nature*, 2005, **433**, 769-773.
20. C. G. Liu, G. A. Calin, B. Meloon, N. Gamliel, C. Sevignani, M. Ferracin, C. D. Dumitru, M. Shimizu, S. Zupo, M. Dono, H. Alder, F. Bullrich, M. Negrini and C. M. Croce, *Proc. Natl. Acad. Sci. U.S.A.*, 2004, **101**, 9740-9744.
21. C. Chen, D. A. Ridzon, A. J. Broomer, Z. Zhou, D. H. Lee, J. T. Nguyen, M. Barbisin, N. L. Xu, V. R. Mahuvakar, M. R. Andersen, K. Q. Lao, K. J. Livak and K. J. Guegler, *Nucleic Acids Res.*, 2005, **33**, e179.
22. C. K. Raymond, B. S. Roberts, P. Garrett-Engele, L. P. Lim and J. M. Johnson, *RNA*, 2005, **11**, 1737-1744.
23. R. Shi and V. L. Chiang, *Biotechniques*, 2005, **39**, 519-525.
24. C. Y. Yu, B. C. Yin and B. C. Ye, *Chem. Commun.*, 2013, **49**, 8247-8249.
25. H. Jia, Z. Li, C. Liu and Y. Cheng, *Angew. Chem., Int. Ed.*, 2010, **49**, 5498-5501.
26. B. C. Yin, Y. Q. Liu and B. C. Ye, *J. Am. Chem. Soc.*, 2012, **134**, 5064-5067.
27. Y. Zhang and C. Y. Zhang, *Anal. Chem.*, 2012, **84**, 224-231.
28. R. Duan, X. Zuo, S. Wang, X. Quan, D. Chen, Z. Chen, L. Jiang, C. Fan and F. Xia, *J. Am. Chem. Soc.*, 2013, **135**, 4604-4607.
29. C. Li, Z. Li, H. Jia and J. Yan, *Chem. Commun.*, 2011, **47**, 2595-2597.
30. Y. Zhang and C.-y. Zhang, *Anal. Chem.*, 2011, **84**, 224-231.
31. X. P. Wang, B. C. Yin, P. Wang and B. C. Ye, *Biosens. Bioelectron.*, 2013, **42**, 131-135.
32. D. A. Shagin, D. V. Rebrikov, V. B. Kozhemyako, I. M. Altshuler, A. S. Shcheglov, P. A. Zhulidov, E. A. Bogdanova, D. B. Staroverov, V. A. Rasskazov and S. Lukyanov, *Genome Res.*, 2002, **12**, 1935-1942.
33. C. A. Mirkin, R. L. Letsinger, R. C. Mucic and J. J. Storhoff, *Nature*, 1996, **382**, 607-609.
34. W. Xu, X. Xue, T. Li, H. Zeng and X. Liu, *Angew. Chem., Int. Ed.*, 2009, **48**, 6849-6852.
35. J. Liu and Y. Lu, *Angew. Chem. Int. Ed.*, 2005, **45**, 90-94.
36. D. Li, A. Wieckowska and I. Willner, *Angew. Chem. Int. Ed.*, 2008, **47**, 3927-3931.
37. H. Li and L. Rothberg, *Proc. Natl. Acad. Sci. U. S. A.*, 2004, **101**, 14036-14039.
38. Y. Wang, F. Yang and X. Yang, *Biosens. Bioelectron.*, 2010, **25**, 1994-1998.
39. J. S. Lee, P. A. Ulmann, M. S. Han and C. A. Mirkin, *Nano Lett.*, 2008, **8**, 529-533.
40. C. C. Huang, Y. F. Huang, Z. Cao, W. Tan and H. T. Chang, *Anal. Chem.*, 2005, **77**, 5735-5741.
41. Robert Elghanian, J. J., Storhoff, Robert C. Mucic, Robert L. Letsinger and C. A. Mirkin, *Science*, 1997, **277**, 1078-1081.
42. James J. Storhoff, Robert Elghanian, Robert C. Mucic, Chad A. Mirkin and R. L. Letsinger, *J. Am. Chem. Soc.*, 1998, 1959-1964.
43. Y. Zu and Z. Gao, *Anal. Chem.*, 2009, **81**, 8523-8528.
44. B. C. Yin, Y. Q. Liu and B. C. Ye, *Anal. Chem.*, 2013, **85**, 11487-11493.
45. C. Y. Yu, B. C. Yin and B. C. Ye, *Chem. Commun.*, 2013, **49**, 8247-8249.
46. F. T. Zhao, Y. Zhou, Y. X. Zhou, Q. Yang, L. Song, X. J. Jiang and Z. S. Jia, *Med. Sci. Monit.*, 2015, **21**.